JOURNAL OF PHYSICAL ORGANIC CHEMISTRY
J. Phys. Org. Chem. 2007; **20:** 589–593
Published online in Wiley InterScience
(www.interscience.wiley.com) DOI: 10.1002/poc.1211

Hydrazide-based non-symmetric liquid crystal dimers: synthesis and mesomorphic behavior

Binglian Bai, Haitao Wang, Hong Xin, Jianhua Shi, Beihong Long and Min Li*

Key Laboratory for Automobile Materials (JLU), Ministry of Education, Institute of Materials Science and Engineering, Jilin University, Changchun 130012, People's Republic of China

Received 13 February 2007; revised 24 March 2007; accepted 31 March 2007

ABSTRACT: Hydrazide-based non-symmetric liquid crystal dimers were synthesized. The liquid crystalline properties were investigated by differential scanning calorimetry (DSC), polarizing optical microscopy (POM), and powder X-ray diffraction (XRD). These non-symmetric liquid crystal dimers are evidenced to display the monolayer smectic C phase. The effects of the lateral intermolecular hydrogen bonding as well as the length of the terminal alkyl chains and the spacers on the mesophase are discussed. Our studies reveal that intermolecular hydrogen bonding between the hydrazide groups and microsegregation effect is the driving force for the formation of the monolayer smectic C structure. Copyright © 2007 John Wiley & Sons, Ltd.

KEYWORDS: liquid crystal dimers; intermolecular hydrogen bonding; smectic phase; microphase segregation; monolayer

INTRODUCTION

In recent years liquid crystal dimers[1–3] (also known as dimesogens), composed of either two identical (symmetric) or non-identical (non-symmetric) mesogenic units connected via a flexible central spacer, have attracted attention not only because they are regarded as model compounds for polymeric liquid crystals[2,3] but also due to their inherently interesting liquid crystalline properties.[4,5]

There are remarkable differences in the behavior of non-symmetric and symmetric dimers. For the majority of symmetric dimers containing terminal alkyl chains, a simple empirical rule has emerged relating the occurrence of smectic behavior to the molecular structure; specifically, if a symmetric dimer is to exhibit a smectic phase then the terminal chain length must be greater than half the spacer length.[1–3,6] Symmetric dimers appear therefore to have a strong tendency to exhibit monolayer smectic phases which is due to the incompatibility between the terminal alkyl chains and the spacers, leading to a microphase separation into three regions: terminal chains, mesogenic groups, and flexible alkyl spacers.[3] In contrast, non-symmetric liquid crystal dimers often exhibit intercalated smectic phases, in which specific molecular interactions between the two different mesogenic units account for this specific phase behavior.[1–3,7,8]

It is well known that intermolecular hydrogen bonding plays an important role in mesophase formation in the hydrazide derivatives; for example, linear *N*,*N*′-bis (4-alkoxybenzoyl)hydrazines exhibit a cubic phase,[9–11] while monomeric, dimeric, and polymeric *N*,*N*′-bis [3,4,5-tris(alkoxybenzoyl)]hydrazines form a columnar phase.[11,12] Recently, we have demonstrated that lateral intermolecular hydrogen bonding was still interacting in the SmA phase and played an important role in stabilizing the mesophase of non-symmetric hydrazide derivatives.[13] We have also demonstrated that lateral intermolecular hydrogen bonding was the driving force for the intercalated smectic phase in symmetric liquid crystal dimers composing of hydrazide groups.[14] If we introduce lateral intermolecular hydrogen bonding into non-symmetric liquid crystal dimers, along with the interaction between the identical mesogenic units in non-symmetric dimers, do they still exhibit intercalated smectic phases dimers? To investigate this, we have designed a series of non-symmetric liquid crystal dimers containing alkoxy benzoyl hydrazine and azobenzene group as the mesogenic units (see Scheme 1), in which the lateral intermolecular hydrogen bonding was expected to increase the intermolecular interaction and both the spacer and terminal chain length were varied with a view to stabilizing different mesophases and understanding structure property relationships.

**Correspondence to:* M. Li, Key Laboratory for Automobile Materials (JLU), Ministry of Education, Institute of Materials Science and Engineering, Jilin University, Changchun 130012, People's Republic of China.
E-mail: minli@mail.jlu.edu.cn

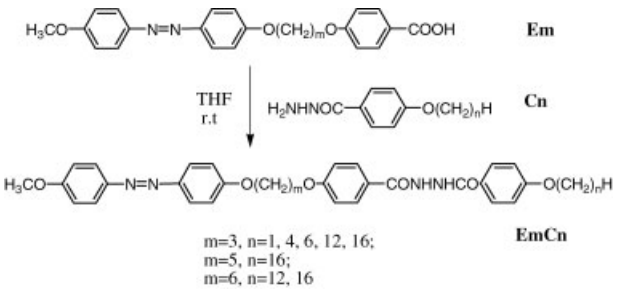

Scheme 1. The synthetic routes for **EmCn**

Here, we report the synthesis, phase behavior, and mesophase structures of 1-[4-(4′-methoxyphenylazo) phenoxyl]-*m*-[(*N*-(4-alkoxybenzoyl)-*N*′-(benzoyl-4′-oxy) hydrazine)] alkane (**EmCn**) (see Scheme 1).

EXPERIMENTAL

Synthesis

The target non-symmetric dimers, abbreviated as **EmCn** (where **m** signifies the number of methylene units in the spacer and **n** indicates the length of terminal alkoxy tail), were synthesized through the route shown in Scheme 1. 4-{*m*-[4-(4-Methoxyphenylazo)phenoxy]alkoxy}benzoic acid (**Em**) was first prepared as described in Ref. 15, the target products were obtained through the reaction of 4-{*m*-[4-(4-methoxyphenylazo)phenoxy]alkoxy}benzoic chloride and 4-alkoxy benzoyl hydrazine (**Cn**) in tetrahydrofuran at room temperature using pyridine as catalyst. The compounds **E6C12** and **E6C16** were purified by recrystallization from DMF, and **E3Cn**, **E5C16** were purified by recrystallization from THF for further ^{1}H NMR measurements, FT-IR and elemental analysis. (Because of the poor solubility, ^{1}H NMR measurement of **E6Cn** did not perform.)

1-[4-(4′-Methoxyphenylazo)phenoxyl]-3-[(*N*-(4-methyloxybenzoyl)-*N*′-(benzoyl-4′-oxy)hydrazine)]propane (E3C1). 4-{3-[4-(4-Methoxyphenylazo) phenoxy]propyloxy}benzoic acid (**E3**, 0.009 mol) and thionyl chloride (20 ml) were refluxed for 5 h. 4-{3-[4-(4-Methoxyphenylazo)phenoxy]propyloxy}benzoic chloride was collected after removing the unreacted thionyl chloride. Then, 4-{3-[4-(4-methoxyphenylazo) phenoxy]propyloxy}benzoic chloride and 4-methoxy benzoyl hydrazine (0.009 mol) were dissolved in tetrahydrofuran (100 ml), pyridine (5 ml) was added, and the resulting mixture was stirred at room temperature for 8 h. The reaction mixture was poured into an excess of ice water and the precipitate recrystallized from tetrahydrofuran.

^{1}H NMR (300 MHz, DMSO) (ppm, from TMS): 2.25–2.26 (m, 2H, —C—CH_2—C—), 3.83–3.86 (d, 6H, —Ar—O—CH_3), 4.26–4.27 (m, 4H, —O—CH_2—C—), 7.04–7.10 (m, 4H, Ar—H, m-to, —CON—), 7.11–7.17 (m, 4H, Ar—H, m-to, —N═N—), 7.83–7.86 (m, 4H, Ar—H, o-to, —N═N—), 7.90–7.92 (m, 4H, Ar—H, o-to, —CON—), 10.30 (s, 2H, —CO—NH—NH—CO—).

FT-IR (KBr, pellet, cm^{-1}): 3224, 2946, 2840, 1674, 1642, 1599, 1581, 1561, 1516, 1499, 1466, 1311, 1251, 1179, 1148, 1106, 1058, 1028, 841, 749.

Anal. calcd for $C_{31}H_{30}N_4O_6$: C, 67.14; N, 10.10; H, 5.45. Found: C, 66.80; N, 10.10; H, 5.45.

Using the same method, compounds **E3C4**, **E3C6**, **E3C12**, **E3C16**, **E5C16**, **E6C12**, and **E6C16** were successfully synthesized and characterized. **E3C4**, Anal. calcd for $C_{34}H_{36}N_4O_6$: C, 68.44; N, 9.39; H, 6.08. Found: C, 68.55; N, 9.55; H, 6.19. **E3C6**, Anal. calcd for $C_{36}H_{40}N_4O_6$: C, 69.21; N, 8.97; H, 6.45. Found: C, 68.87; N, 8.80; H, 6.66. **E3C12**, Anal. calcd for $C_{42}H_{52}N_4O_6$: C, 71.16; N, 7.90; H, 7.39. Found: C, 70.80; N, 7.88; H, 7.64. **E3C16**, Anal. calcd for $C_{46}H_{60}N_4O_6$: C, 72.22; N, 7.32; H, 7.91. Found: C, 72.00; N, 7.41; H, 8.08. **E5C16**, Anal. calcd for $C_{48}H_{64}N_4O_6$: C, 72.70; N, 7.06; H, 8.13. Found: C, 72.60; N, 6.96; H, 8.21. **E6C12**, Anal. calcd for $C_{45}H_{58}N_4O_6$: C, 71.97; N, 7.46; H, 7.78. Found: C, 71.84; N, 7.40; H, 7.85. **E6C16**, Anal. calcd for $C_{49}H_{66}N_4O_6$: C, 72.92; N, 6.94; H, 8.24. Found: C, 73.08; N, 6.59; H, 8.43.

Characterization

^{1}H NMR spectra were recorded with a Mercury-300BB 300 MHz spectrometer, using DMSO-d6 as solvent and tetramethylsilane (TMS) as an internal standard. FT-IR spectra were recorded with a Perkin-Elmer spectrometer (Spectrum One B), using KBr pellets. The thermal properties of the compounds were investigated with a Mettler-Toledo DSC821^e instrument. The rate of heating and cooling was 10 °C min^{-1}, the weight of the sample was about 2 mg, and indium and zinc were used for calibration. The peak maximum was taken as the phase transition temperature. Optical textures were observed by polarizing optical microscopy (POM) using a Leica DMLP microscope equipped with a Leitz 350 heating stage. X-ray diffraction (XRD) was carried out with a Bruker Avance D8 X-ray diffractometer.

RESULTS AND DISCUSSION

Intermolecular hydrogen bonding in EmCn

We have demonstrated that the lateral intermolecular hydrogen bonding was still interacting in the SmA phase of hydrazide derivatives.[13] In order to explore whether the intermolecular hydrogen bonding exists in these liquid crystal dimers, temperature-dependent FT-IR spectra were performed. Take the compound **E6C16**, for example, the presence of —NH stretching vibrations at

DOI: 10.1002/poc

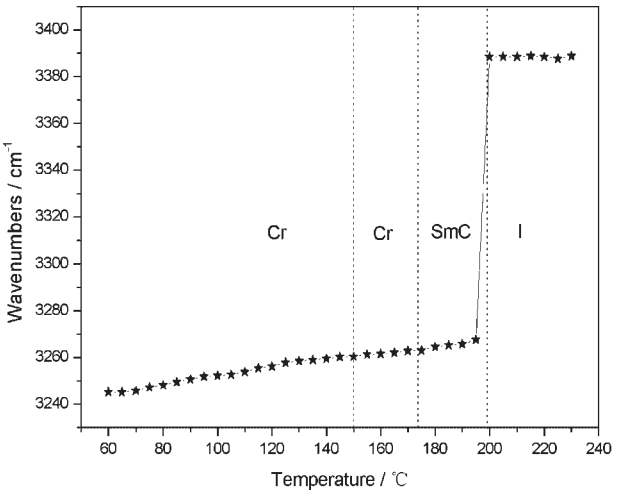

Figure 1. The temperature dependent –NH stretching vibrations of **E6C16** on first cooling: Cr, SmC, and I indicate crystalline state, smectic C phase, and isotropic state, respectively

3245 cm^{-1}, intense absorption of amide I at 1675, 1653 cm^{-1} clearly indicated that almost all the —NH groups are associated with —C═O groups via —N—H. . .O═C— hydrogen bonding[13] at room temperature. The wavenumbers of —NH stretching vibration of **E6C16** are around 3245, 3265, and 3300 cm^{-1} (very weak) in the crystalline state, SmC phase, and isotropic phase, respectively, and in isotropic phase a strong sharp peak around 3387 cm^{-1} was observed. The observed —NH stretching vibration frequency at 3265 cm^{-1} in the SmC phase and the increase of —NH stretching vibration by *ca.* 122 cm^{-1} at the isotropic transition strongly indicated the presence of the hydrogen bonding in the SmC phase of **E6C16**. Fig. 1 shows the temperature dependence of ν (—NH) of **E6C16**. A sharp increase of ν (—NH) wavenumbers on going from liquid crystalline phase to isotropic liquid was noticed.

Phase behavior

The phase behavior of **EmCn** was studied by polarized optical microscopy (POM), differential scanning calorimetry (DSC), and powder XRD. The compounds **E6C12** and **E6C16** show enantiotropic smectic C with schlieren textures, as shown in Fig. 2a. The compounds **E3C12**, **E5C16**, and **E3C16** exhibit monotropic smectic C phase in which schlieren coexistence with fan-like texture or schlieren textures were observed (Fig. 2b), and the broken fan-shaped texture (Fig. 2c), which on shearing gives a schlieren texture. The compound **E3C1** shows monotropic nematic phase, its optical texture showed the high mobility which flashes when subjected to mechanical stress (Fig. 2d). However, no mesophase was observed for **E3C4** and **E3C6**.

Their transitional temperatures and associated enthalpies were summarized in Table 1. It can be seen that

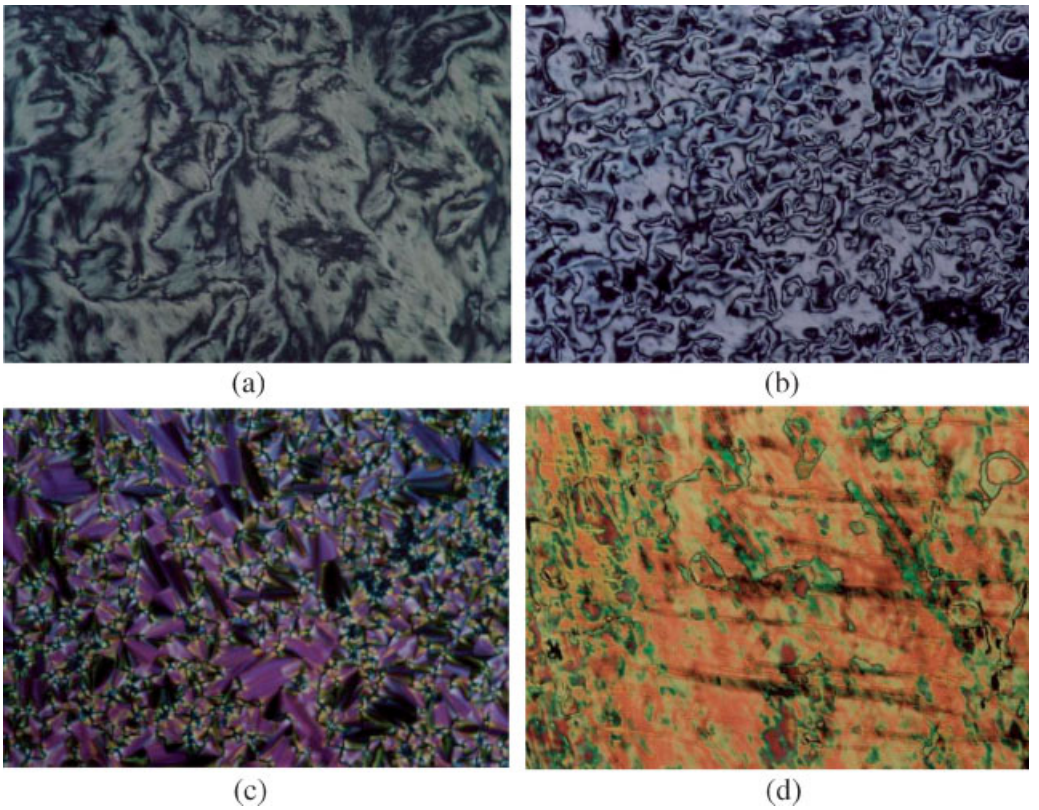

Figure 2. Polarizing optical photomicrograph of **E6C16**, **E5C16**, **E3C1**, and **E3C16**. (a) Schlieren texture of **E6C16** at 188 °C (200×); (b) schlieren textures of **E5C16** at 157 °C (200×); (c) broken fan-shaped texture of **E3C16** at 155.6 °C (400×); (d) nematic texture of **E3C1** at 168 °C (200×).

DOI: 10.1002/poc

Table 1. Transition temperatures (°C) and enthalpies (kJ mol^{-1}, in parentheses) of **EmCn**

Compound	First cooling	Second heating
E3C1	I 181 (1.2) N 151 (39.7) Cr	Cr 196 (52.2) I
E3C4	I 172 (47.6) Cr 93 (0.5) Cr	Cr 186 (47.7) I
E3C6	I 173 (51.1) Cr	Cr 187 (55.1) I
E3C12	I 175 (6.8) SmC 153 (39.5) Cr	Cr 174 (2.4) Cr 183 (50.7) I
E3C16	I 168 (5.26) SmC 151 (30.7) Cr 134 (2.2) Cr 106 (4.74) Cr	Cr 109 (5.3) Cr 176 (34.7) I
E5C16	I 169 (8.4) SmC 147 (36.9) Cr 116 (1.2) Cr	Cr 119 (1.0) Cr 141 (20.0) Cr 170 (47.7) I
E6C16	I 199 (14.6) SmC 177 (42.7) Cr 156 (16.7) Cr	Cr 188 (74.6) SmC 201(14.1) I
E6C12	I 195 (13.3) SmC 172 (39.3) Cr	Cr 183 (42.7) SmC 196 (12.6) I

Cr, SmC, and I indicate crystalline state, smectic C phase, and isotropic liquid, respectively.

length of the terminal alkyl chains plays an important role in the formation of the mesophase. Compounds **E3Cn** with long alkyl chain such as **E3C12** and **E3C16** exhibited monolayer SmC phase, whereas nematic phase for **E3C1** and non-mesomorphic for **E3C4** and **E3C6**. Both the melting and clearing points of **E5C16** are much lower than those of **E6C16**, which indicated the characteristic odd–even effect in **EmCn**, as usually observed in liquid crystal dimers.[1,3]

Mesophase structure of EmCn

In order to obtain further information on molecular arrangements in their mesophase, variable temperature XRD was performed on **EmCn**. A characteristic pattern of the nematic phase was observed in the mesophase of **E3C1**. The XRD pattern of **E6C16** in the smectic phase contains two sharp peaks in the low-angle region implying the formation of a layered structure, and a broad diffuse peak in the wide-angle region centered at a spacing of 4.6 Å, indicating liquid-like arrangement of the molecules within the layers, as shown in Fig. 3. The layer spacing (*d*) is 50.42 Å, which is a little bit smaller than the estimated all-trans molecular length (*l*) of the most extended conformation of 56.56 Å, considering its schlieren texture, indicating that the molecules of **E6C16** are arranged in a monolayer with the molecular long axis tilted with respect to the layer normal (SmC). So we can propose that the molecules should have the ordering with alternating orientations of the mesogens, as shown in Fig. 4, in which the azobenzene part can be considered more or less as a part of one of the tails, while the hydrazide-containing segment as the rigid core that is quite close to the center of the molecules. Moreover, this packing model is in favor of formation of intermolecular hydrogen bonding between the hydrazide-containing groups, which was confirmed through variable temperature FT-IR experiments. Similar molecular arrangements were observed for compounds **E3C16**, **E3C12**, **E5C16**, and **E6C12** in their SmC phase; data for *d*, *l*, and *d*/*l* ratios are collected in Table 2.

An intercalated smectic phase has generally been observed in non-symmetric liquid crystal dimers, and it is accepted that special interaction between the different

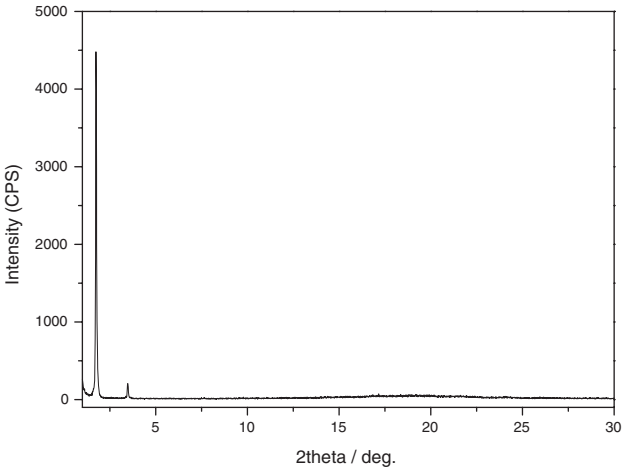

Figure 3. X-ray diffraction (XRD) pattern of **E6C16** at 190 °C

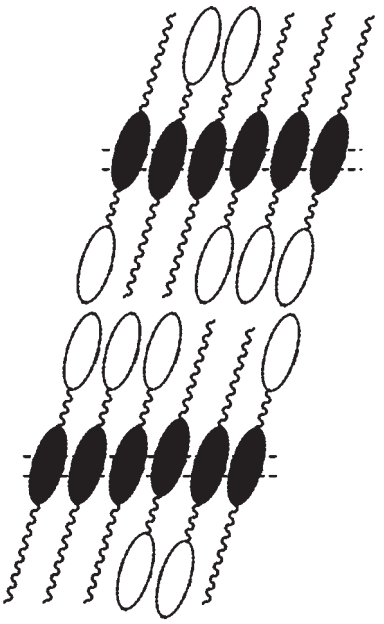

Figure 4. A sketch of the monolayer smectic C of **E6C16** (the dashed lines indicate the lateral hydrogen bonding between mesogens, ellipse and filled ellipse represent different mesogenic groups)

DOI: 10.1002/poc

Table 2. Summary of XRD results for **EmCn** in their mesophases

Compounds	Molecular length[a] l (Å)	T (°C)	Layer spacing d (Å)	d/l
E6C16	56.56	190	50.42	0.89
E6C12	51.95	190	46.14	0.89
E3C12	48.35	160	38.05	0.79
E3C16	53.39	160	43.23	0.82
E5C16	55.83	160	44.57	0.80

[a] Molecular length was calculated by MM2.

mesogenic moieties is responsible for the specific structure.[1–3] It is true that long terminal alkyl chains will cause microphase segregation in **EmCn** and thus favor the formation of layer structure, while the onset of lateral hydrogen bonding between hydrazide groups facilitate tilting of the mesogenic groups as well as monolayer arrangement. Thus, the monolayer SmC phase of **EmCn** with long terminal chains was due to the combined effect of microphase segregation and the lateral hydrogen bond. Especially, in the present non-symmetric dimers, lateral hydrogen bond between the same kinds of mesogenic groups plays an important role for the formation of monolayer structure, which has been demonstrated to be the driving force for the intercalated smectic phase in symmetric liquid crystal dimers composing of hydrazide groups as reported previously by us.[14] The present results showed that it was possible to fine-tune the molecular arrangement through introducing specific lateral intermolecular interactions and controlling the balance among different interactions.

CONCLUSION

In the present study, we have introduced intermolecular hydrogen bonding into non-symmetric liquid crystal dimers, by choosing the hydrazide group in the mesogenic units; and monolayer smectic C phases in these non-symmetric dimers were observed. The lateral hydrogen bonding between the hydrazide groups and microsegregation effect was the driving force for the formation of the monolayer smectic C structure. The lengths of terminal alkyl chains also play key roles in the formation of the stable smectic phase.

Acknowledgements

The authors are grateful to the National Science Foundation Committee of China (project No. 50373016), Program for New Century Excellent Talents in Universities of China Ministry of Education, Special Foundation for PhD Program in Universities of China Ministry of Education (Project No. 20050183057), and Project 985-Automotive Engineering of Jilin University for their financial support of this work.

REFERENCES

1. Imrie CT, Luckhurst GR. *Handbook of Liquid Crystals*, In vol. 2B, Demus D, Goodby JW, Gray GW, Spiess HW, Vill V (eds). Wiley-VCH: Weinheim, 1998.
2. (a) Imrie CT, Henderson PA. *Curr. Opin. colloid. inter. Sci.* 2002; **7**: 298–311; (b) Šepelj M, Lesac A, Baumeister U, Diele S, Bruce DW, HamerŠak Z. *Chem. Mater.* 2006; **18**: 2050–2058; (c) Lee WK, Kim KN, Achard MF, Jin JI. *J. Mater. Chem.* 2006; **16**: 2289–2297.
3. Imrie CT. *Struct. Bond.* 1999; **95**: 149–191.
4. Weissflog W, Lischka CH, Diele S, Wirth I, Pelzl G. *Liq. Cryst.* 2000; **27**: 43–50.
5. Krishnan K, Balagurusamy VSK. *Liq. Cryst.* 2001; **28**: 321–325.
6. (a) Date RW, Imrie CT, Luckhurst GR, Seddon JM. *Liq. Cryst.* 1992; **12**: 203–238; (b) Takemoto M, Mori A, Ujiie S, Vill V. *Liq. Cryst.* 2002; **29**: 687–695.
7. (a) Hogan JL, Imrie CT, Luckhurst GR. *Liq. Cryst.* 1988; **3**: 645–650; (b) Lee DW, Jin JI, Laguerre M, Achard MF, Hardouin F. *Liq. Cryst.* 2000; **27**: 145–152.
8. (a) Attard GS, Date RW, Imrie CT, Luckhurst GR, Roskilly SJ, Seddon JM, Taylor L. *Liq. Cryst.* 1994; **16**: 529–581; (b) Wallage MJ, Imrie CT. *J. Mater. Chem.* 1997; **7**: 1163–1167.
9. Demus D, Gloza A, Hauser H, Rapthel I, Wiegeleben A. *Cryst. Res. Technol.* 1981; **16**: 1445–1451.
10. Kutsumizu S. *Curr. Opin. solid state mater. Sci.* 2002; **6**: 537–543.
11. Beginn U. *Prog. polym. Sci.* 2003; **28**: 1049–1105.
12. Beginn U, Lattermann G, Festag R, Wendorff JH. *Acta. Polym.* 1996; **47**: 214–218.
13. Pang DM, Wang HT, Li M. *Tetrahedron* 2005; **61**: 6108–6114.
14. Wang HT, Bai BL, Zhang P, Long BH, Tian WJ, Li M. *Liq. Cryst.* 2006; **33**: 445–450.
15. Bai BL, Wang HT, Xin H, Long BH, Li M. *Liq. Cryst.* 2007; DOI: 10.1080/02678290701328118.